

Modeling the Mechanical Properties of Highly Oriented Polymer Films: A Fiber/Gel Composite Theory Approach

D. RYAN BREESE,* GREGORY BEAUCAGE

Department of Chemical and Materials Engineering, University of Cincinnati, Cincinnati, Ohio 45221

Received 31 August 2007; accepted 29 November 2007

DOI: 10.1002/polb.21396

Published online in Wiley InterScience (www.interscience.wiley.com).

ABSTRACT: Controlling the extent of orientation is of great interest in polymer processing and is effected by the choice of polymer, the fabrication technique and the processing conditions. Understanding the crystalline transitions that form highly oriented fibrils is necessary for modeling the changes in physical properties, relative to degree of orientation. A model is proposed to describe the mechanical properties of drawn semicrystalline polymer films based on structural transitions. With a minimal amount of experimental data (requiring testing on only two drawn films samples), this model can be used to predict film properties. These properties include the critical and maximum draw ratios, the moduli at the maximum draw ratio, the moduli of the fiber, the modulus of the nonfibrous gel relative to draw ratio, the volume fraction of fibers, and the rate of fibrillation. Where high degrees of uniaxial orientation are required, the polymer is typically drawn in the solid state, meaning the polymer is stretched in a single direction at temperatures below the melting point. During this process, pre-existing crystallites are transformed into fiber-like structures with large aspect ratios. The presence of these rigid asymmetric structures significantly enhances the moduli and break strength of the polymer. This work presents a model that describes the formation of fiber-like structures. The volume fraction of fibers is predicted to be linear in draw ratio. The derived relationship between volume fraction of fibers and draw ratio can then be used for the prediction of the various properties of the oriented film.

©2008 Wiley Periodicals, Inc. *J Polym Sci Part B: Polym Phys* 46: 607–618, 2008

Keywords: films; modeling; MDO; orientation; phase behavior; structure-property relations; uniaxial

INTRODUCTION

Polymer films can be oriented to improve their physical properties such as the modulus and tensile strength. Several approaches have been proposed to explain the molecular transitions that occur during orientation, but none combine the dynamics of fibrillation and how it relates to measurable physical properties.¹ These models

range from mechanical^{2–4} to more elaborate structural composite models consisting of fibers of finite length^{5,6} that when oriented form fibrillar structures,⁷ fibers whose aspect ratio increases upon orientation,⁸ and elaborate hierarchical systems consisting of fibrous structures of taut tie molecules on several length scales.^{9–11}

A mechanical model that explains the dynamics of the polymer structural changes is needed for relating the enhancements in the physical properties to the degree of orientation. In this article, a generalized model is proposed that uses measured macroscopic physical properties and fiber composite theory to create a fundamental understanding of structure-property

*Present address: Eclipse Film Technologies, Hamilton, OH 45011.

Correspondence to: D. R. Breese (E-mail: rbreese@eclipsefilmttech.com)

Journal of Polymer Science: Part B: Polymer Physics, Vol. 46, 607–618 (2008)
©2008 Wiley Periodicals, Inc.

relationships that can be used to produce oriented semicrystalline polymer films with improved mechanical properties. The proposed transition model is similar to that of Weeks and Porter¹² and Gibson et al.⁷ (which utilized Cox's shear lag theory¹³), but is improved in the sense that the effects of the orientation process on the modulus of the nonfibrous gel component are incorporated into the model by allowing a transition to fibers. In the case of Weeks and Porter's sheath and core model,¹² they neglect any changes in the morphology of the sheath. For the short fiber model of Halpin and Kardos⁵ or the shear-lag based models of Gibson et al.⁷ and Barham and Arridge,⁸ knowledge of a finite aspect ratio of the fibers is necessary, while changes in the structure of the matrix for the composite are ignored. In addition, once the fibers are formed, further orientation does little to enhance the fiber's contribution to the composite.⁵

Transient characteristics of semicrystalline polymers, such as degree of crystallinity and lamellar thickness, were avoided as parameters for the model as they are sensitive to variations in processing conditions, such as level of orientation. Most commonly, the percent crystallinity increases with increasing orientation.¹⁴⁻²⁵ In the case of polymer films, a highly oriented polymer of low crystallinity can have a significantly higher modulus than an unoriented polymer of higher crystallinity,^{19,26} but if the level of orientation were the same, the highly crystalline polymer would have a greater modulus than the lower crystalline polymer.^{19,27-29} To the contrary, processing conditions can at times be set such that the bulk percent crystallinity decreases with increasing levels of orientation.^{3,20}

These transient polymer characteristics are related to the properties specific to the structural entities in this model (fiber and nonfibrous gel) and as a result, govern the ultimate values of the oriented polymer, but not the mechanics by which the structure was created. Such properties of the structural components of the model include the machine and transverse direction moduli of the fiber ($E_{f,MD}$ - eq 3, $E_{f,TD}$ - eq 5) and the modulus of the nonfibrous gel (E_{NF} - eqs 3 and 5) and will serve as the key parameters for this model.

The following transitional model is a simple and practical way of predicting the physical properties of oriented polymer films at a wide range of operating conditions. Detailed informa-

tion about the structure and properties of oriented films can be obtained by conducting commonly utilized mechanical property testing on a minimal amount of experimental samples.

TRANSFORMATIONAL MODEL

A two domain system (anisotropic semicrystalline fibers and less ordered semicrystalline gel-like physical network) each consisting of amorphous and crystalline phases can be used to model oriented films. The two types of domains are distinguishably different, as shown in Figure 1, a schematic of the fiber/nonfibrous gel system.

At the initial condition for the high density polyethylene, the lamellae are of a Keller-Machin 1 (low stress) morphology,³⁰ which is typical for blown high density polyethylene films.³¹ At this condition, the volume fraction of fibers oriented in the machine direction is negative. This is the result of the crystallographic orientation of the unit cell, with the a -axis more preferentially oriented in the machine direction, the b -axis more preferentially oriented in the transverse direction and the c -axes more preferentially oriented in the normal direction.³¹ Such morphology results in the transverse direction modulus being slightly greater than the machine direction modulus. This corresponds to a low, negative volume fraction of fibers relative to the machine direction. This morphology is the direct result of the film fabrication process. Different film fabrication techniques, such as quenching a uniaxially strained melt (cast film) or isotropically strained crystallization, may not display a negative volume fraction of fibers. Recent work with oriented Nafion films has shown similar behavior when deformed perpendicular to the "preoriented" direction.³²

At the critical draw ratio, indicated by isotropic mechanical properties, preorientation from the film fabrication process has been erased and the machine and transverse direction moduli are equal, resulting in the calculated volume fraction of fibers in either direction equal to 0%. At low machine direction orientation levels, the crystallites are positioning for the transformation from a Keller-Machin 1 morphology to a Keller-Machin 2 morphology. As the level of orientation increases, the less rigid components of the nonfibrous gel become ordered and begin to form fibrous structures. Fibrillation continues through moderately high levels of orientation, where the tie molecules are pulled

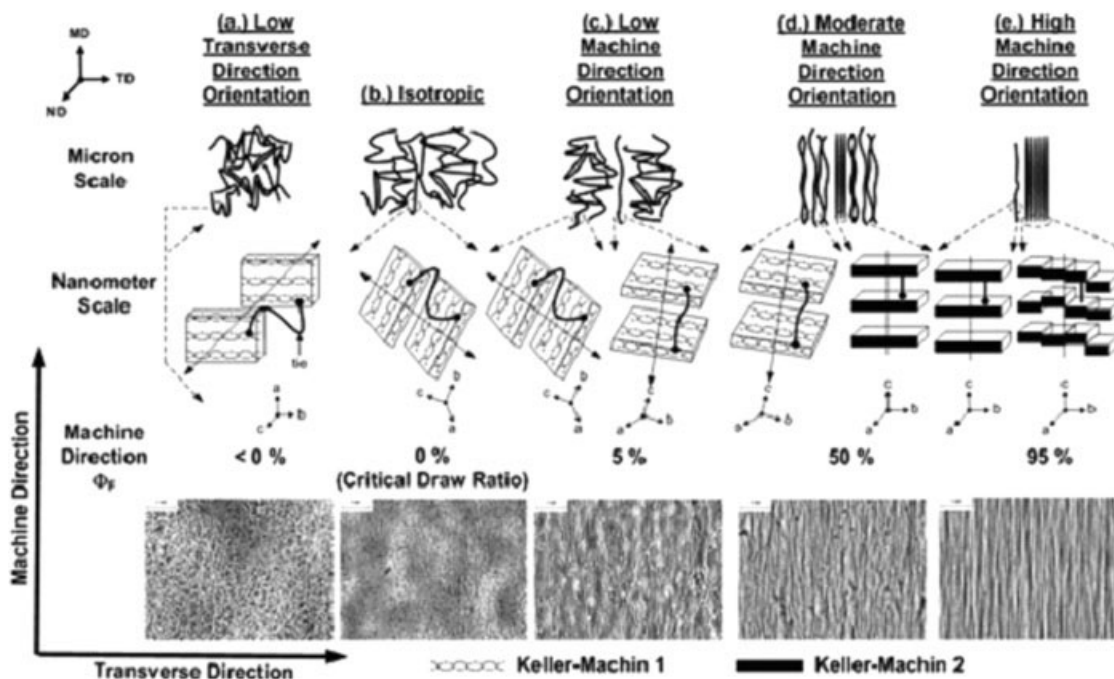


Figure 1. Schematic of the fibrous and nonfibrous gel domains on the micron and nanometer length scales. Each of the sketches shows a low magnification (top) and high magnification (bottom) perspective. Included at the bottom of the figure are optical microscopic images collected from high density polyethylene film samples at the various stages in the orientation process. For the high magnification, the anisotropic entities aligned in a specified direction represent the crystalline component of the fibrous structures, such as lamellae oriented parallel to each other, forming stacks connected with tie molecules. The amorphous component is represented by the voids between the crystalline components. A single interlamellar tie molecule is shown to represent the changes that occur to the tie molecule during deformation.

taunt and the Keller-Machin 1 morphologies are converted to Keller-Machin 2 (high strain) morphologies. In the high strain morphology, the a -axis of the unit cell is oriented in the normal direction, the b -axis is oriented in the transverse direction and the c -axis is oriented in the machine direction. At this point, large scale fibers begin to form. At high draw ratios, lamellae fracture along the $\langle 001 \rangle$,³³ forming a stair-step morphology.³⁴ Finally, the maximum draw ratio is reached, where all of the nonfibrous components have been converted into fibrous structures. This condition is indicative of a volume fraction of fibers equal to unity.

The fibrous domains contain uniaxially oriented stacks of lamellae and what lamellae that may have unraveled to form extended chains, interconnected by tie molecules and entanglements, some of which may be taunt.^{35–37} The second domain, the nonfibrous gel, contains less ordered lamellae which are also interconnected

with loose tie molecules and entanglements. Defects, such as chain ends, tie molecules, entanglements, and mosaic boundary layers account for each domain's respective amorphous fraction.⁹ In both domains, polydispersity in lamellar size, perfection, and stacking (ordering) is assumed.³⁸

On the micron scale, the crystallites of the fiber portion have a very large aspect ratio relative to the crystallites of the nonfibrous gel portion^{27,35,36,39} making the two domains easily distinguishable, both morphologically and in terms of mechanical response.

The sum of the volume fractions of the two semicrystalline domains, the fiber and nonfibrous gel, equals unity.

$$\Phi_F + \Phi_{NF} = 1 \quad (1)$$

where Φ_F is the volume fraction of fiber components and Φ_{NF} is the volume fraction of non-

fibrous gel components. The mechanical response of the system is expected to be determined largely by Φ_F .

Relating the Machine Direction Modulus to the Fiber Volume Fraction

Fibrous structures have been observed by microscopy in oriented polymers.^{27,35,36,39,40} The main issue when applying fiber composite theory to semicrystalline polymers is distinguishing which domain is the “fiber” and which is the “matrix.” The simplest approach would be to model a two domain system consisting of a rigid oriented fibrous domain and a softer matrix.^{2-4,37} Moduli values between 240 and 345 GPa have been reported for the extended polyethylene chain^{8,9,41-43} and moduli values reported in the literature for the amorphous region and unoriented semicrystalline polymers are of two to three orders of magnitude lower than that of the extended chain.^{8,9} It would be presumptuous to assume the idealistic scenario of past models^{7,8} in that the fiber has the modulus of an extended chain and the gel of an amorphous polymer, as we are uncertain that these structures correspond to those seen in the oriented semicrystalline polymers. For the proposed semicrystalline fiber/nonfibrous gel model, the properties for each domain are not assumed to be ideal, since a decrease in the crystallinity of the polymer would result in a decrease in the modulus of both the fibrous and nonfibrous gel components. The relationship between the volume fraction of fibers and the degree of crystallinity is, however, complex and beyond the scope of this model.

From fiber composite theory, the following relationship is used to calculate the machine direction modulus of a fiber composite system with fibers having an extremely large aspect ratio:⁴⁴

$$E_{C,MD} = \sum_{i=1}^n E_{i,MD} \Phi_i \quad (2)$$

where $E_{C,MD}$ is the machine direction modulus of the composite, $E_{i,MD}$ is the modulus of the i th component in the machine direction, and Φ_i is the volume fraction of the i th component.

Halpin and Kardos found that this model reasonably predicts the machine direction modulus of composites with fibers of aspect ratio greater than 10^3 .⁵ By definition, eq 2 is valid for

systems containing fibers that are perfectly oriented in the machine direction, have an extremely large aspect ratio, and when no slippage occurs at the fiber-matrix interface and stress is efficiently transferred between the domains. For polydisperse systems where various domains are miscible and molecular entanglements are present, a no-slip model is assumed. For the case where the fiber aspect ratio is relatively small or interfacial slippage occurs, short fiber composite techniques such as the Halpin-Kardos,⁵ Halpin-Tsai,⁶ and shear-lag based theories^{7,8} could be considered.

For simplicity, eq 2 is used as an approximation for the fiber/nonfibrous gel model and by substitution of eq 1, eq 2 becomes:

$$E_{C,MD} = \Phi_F E_{F,MD} + (1 - \Phi_F) E_{NF} \quad (3)$$

Relating the Transverse Direction Modulus to the Fiber Volume Fraction

From fiber composite theory, the following relationship is used to calculate the transverse direction modulus of a composite system:⁴⁴

$$E_{C,TD} = \frac{1}{\sum_{i=1}^n \frac{\Phi_i}{E_i}} \quad (4)$$

$E_{C,TD}$ is the transverse direction modulus of the composite, E_i is the modulus of the i th component and Φ_i is the volume fraction of the i th component.

Utilizing eqs 1 and 4, an equation for the two component system of fibers and a nonfibrous gel is generated for the transverse direction modulus.

$$E_{C,TD} = \frac{1}{\frac{\Phi_F}{E_{F,TD}} + \frac{(1-\Phi_F)}{E_{NF}}} \quad (5)$$

Close examination of eq 5 supports the two domain fiber/nonfibrous gel model instead of the traditional two phase crystalline/amorphous model. If the latter model were utilized, the lower modulus of the amorphous region would dominate, resulting in a transverse direction modulus of several orders of magnitude lower than the machine direction modulus.^{8,9} In the transitional fiber/nonfibrous gel model, the transverse direction modulus is more equally affected by the moduli of both fiber and gel, primarily due to the semicrystalline nature of both domains. As the orientation increases, the

contribution becomes more balanced, as the volume fraction of fibers increases through the consumption of the gel and the modulus of the gel increases as more flexible components are converted into stiffer fibrous precursors, leaving a concentrate of more rigid components in the gel. Such a relationship explains the observed correlation between the transverse direction modulus and draw ratio.⁴¹

Ultimate Moduli of the Transitional Model

As a polymer film is oriented, the modulus increases linearly in draw ratio until failure due to the completion of the transition of the maximum amount of the nonfibrous gel into fibrous structures at the given orientation conditions (temperature (T) and strain rate ($\dot{\gamma}$)). At this ultimate condition, the highest practically obtainable modulus ($E_{C,MD\ MAX}(T, \dot{\gamma})$) is observed. This concept has a parallel in Peterlin's work,⁹ who states that the fracture of drawn samples in constant rate tensile experiments occurs almost instantaneously as soon as the whole sample has transformed into a fibrous structure.

At this limiting condition, the entire gel domain has been converted into fibers, where we define $\Phi_F = 1$ at $E_{F,MD} = E_{C,MD}$ and eq 2 becomes

$$E_{C,MD\ MAX} = \Phi_{F,MAX} E_{F,MD} \equiv E_{F,MD} \quad (6)$$

This relationship provides an estimate of the machine direction modulus of the fiber, $E_{F,MD}$, for a given polymer, which is assumed to be constant with draw ratio for a given set of intransigent polymer properties and processing conditions.⁸ Equation 6 effectively defines a fiber of a particular polymer sample at ultimate elongation for a given orientation temperature and strain rate.

Substituting $E_{F,MD}$ calculated from eq 6 into eq 3, the following relationship is obtained between the machine direction modulus of a fiber/nonfibrous gel composite with respect to the fiber volume fraction.

$$E_{C,MD} = \Phi_F E_{C,MD\ MAX} + (1 - \Phi_F) E_{NF} \quad (7)$$

where $E_{C,MD}$ is the machine direction modulus of the composite, $E_{C,MD\ MAX}$ is the machine direction modulus of the composite at $\Phi_F = 1$, and E_{NF} is the modulus of the nonfibrous gel component.

On the basis of the same assumptions used to derive eq 6, the transverse direction fiber modulus for a specific polymer and orientation conditions, $E_{F,TD}$, can be calculated by the following equation.

$$E_{C,TD\ MAX} = \frac{1}{\Phi_{F \rightarrow 1} \frac{\Phi_{F,MAX}}{E_{F,TD}}} \equiv E_{F,TD} \quad (8)$$

Substituting the $E_{F,TD}$ calculated from eq 8 into eq 5, the following relationship between the transverse direction modulus of a fiber/nonfibrous gel composite with respect to the fiber volume fraction is obtained.

$$E_{C,TD} = \frac{1}{\frac{\Phi_F}{E_{C,TD\ MAX}} + \frac{(1-\Phi_F)}{E_{NF}}} \quad (9)$$

The model consists of four parameters, the volume fraction of fibers (Φ_F), the maximum modulus in the machine and transverse directions ($E_{C,MD\ MAX}$ and $E_{C,TD\ MAX}$), and the modulus of the nonfibrous gel component (E_{NF}).

The fiber modulus is anisotropic, with significantly higher modulus in the machine direction, relative to the transverse direction. This is because the fiber consists of stacks of lamellae which contain defects and are likely interconnected with tie molecules and entanglements, some of which are taut.⁹⁻¹¹ Such architecture, which consists of strong covalent bonds in the machine direction and weaker van der Waal forces and packing constraints in the transverse direction, gives significant anisotropy in properties.⁹⁻¹¹

COMBINING THE TRANSITIONAL MODEL AND EMPIRICAL FUNCTIONS FOR PREDICTING UNIAXIALLY ORIENTED FILM PROPERTIES

Empirical Relationships between the Machine and Transverse Direction Moduli and the Draw Ratio

The characteristic draw ratio for a film can be defined by the following equation,

$$DR = \frac{t_{undrawn}}{t_{drawn}} = \frac{S_{drawn}}{S_{undrawn}} \quad (10)$$

For an incompressible material, DR is the characteristic draw ratio, $t_{undrawn}$ is the thickness of the undrawn sample, t_{drawn} is the thick-

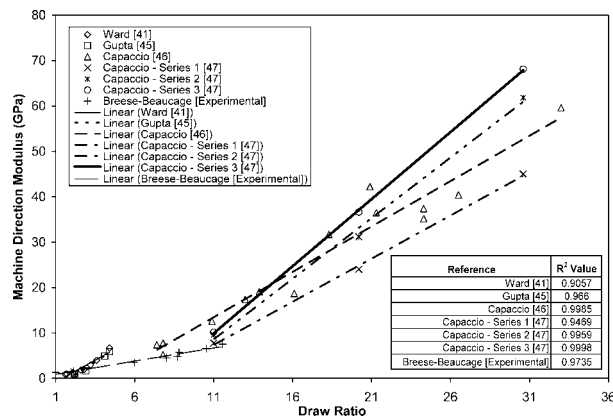


Figure 2. Plot of machine direction modulus versus draw ratio found in the literature^{41,45–47} and recently acquired experimental data. A linear relationship is seen over a wide range of draw ratios, materials and orientation conditions. R^2 values determined from the linear regression of each data set are included.

ness of the drawn sample, S_{drawn} is the surface area of the drawn film, and S_{undrawn} is the surface area of the undrawn film.

Empirical linearly increasing relationships between the machine and transverse direction moduli with the characteristic draw ratio are discussed in the literature.^{41,45–47}

$$E_{C,MD} = M_{MD}(\text{DR}) + B_{MD} \quad (11)$$

M_{MD} and B_{MD} are constants that are specific to the polymer.

$$E_{C,TD} = M_{TD}(\text{DR}) + B_{TD} \quad (12)$$

M_{TD} and B_{TD} are constants that are specific to the polymer.

Similar trends (without the proposed functional relationship) were experimentally shown in the literature for a wide span of draw ratios, ranging from 2 to 33.^{41,45–47} Figure 2 shows the compilation of the machine direction modulus data, relative to changing draw ratio, found in the literature.^{41,45–47} The respective transverse direction modulus is shown in Figure 3.^{41,45}

The different sets of data in Figures 2 and 3 are representative of films of different polymers drawn to various draw ratios. A linear relationship is seen between the modulus and draw ratio for each individual data set. Ward⁴¹ studied LDPE drawn at 20 °C while, Gupta et al.⁴⁵ studied low density polyethylene drawn at 22 °C. The two data sets overlap very closely, with the

marginal differences likely the result of different orientation temperatures and slight differences, though unspecified in the references, in the polymer. Capaccio et al.⁴⁶ studied randomly oriented compression molded samples of ultrahigh molecular weight linear homopolymer polyethylene. This polymer has a melt flow index <0.05 , $M_n = 33,100$ and $M_w = 312,000$. To provide a complete representation of the modulus values over a broad range of draw ratios, the data set associated with this reference in Figure 2 combines values for film samples drawn to various draw ratios at a rate of 10 cm/min and at three different temperatures (105, 110, and 115 °C). Scatter within the data set is the result of combining the data from the three different orientation temperatures into one data set. The higher modulus values, relative to ref. 41 and 46 are the result of the higher molecular weight and crystallinity of Capaccio's samples. Capaccio and Ward⁴⁷ studied pressed homopolymer linear polyethylene samples drawn at a rate of 1 cm/min. The polymer used had a $M_n = 6180$ and $M_w = 101,450$. The modulus was measured by a dead load creep experiment, with measurements taken at various strains, which include: Series 1 = 0.001, Series 2 = 0.002, and Series 3 = 0.005. The deviations between the moduli data of ref. 47, relative to ref. 46, is caused by differences in the molecular weight and the variations in the strains at which the films were tested. Experimental data was collected on an oriented

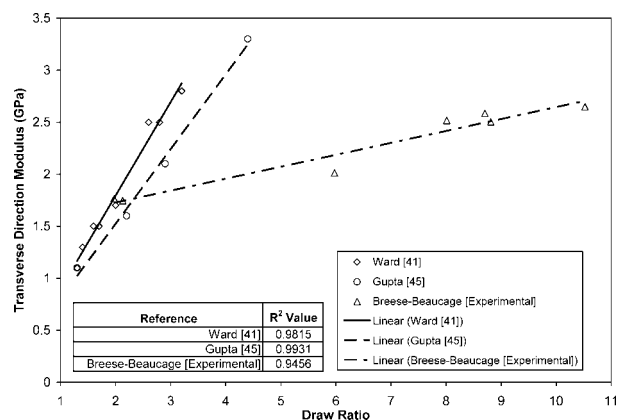


Figure 3. Plot of transverse direction modulus versus draw ratio found in the literature^{41,45} and recently acquired experimental data. A linear relationship is observed relative to increasing draw ratio, as seen with the machine direction modulus. R^2 values determined from the linear regression of each data set are included.

high molecular weight homopolymer polyethylene, with a $M_n = 12,870$ and $M_w = 194,690$. The sample was produced via the blown film process, which has both a slower cooling rate and results in a higher transverse direction orientation, relative to the pressing and quenching process used in the literature. As a result of the differences in sample preparation, as well as those in molecular weight and crystallinity, the modulus data varies from refs. 41, 45–47, but the linear relationship relative to the draw ratio remains consistent with that seen in the literature.

Determining the Volume Fraction of Fibers (Φ_f) from the Moduli (E_{MD} and E_{TD}) of the Oriented Sample

The transitional model predicts the mechanical properties of the polymer sample as a function of Φ_f , which is calculated by first combining eqs 7 and 11 for the machine direction and solving for E_{NF}

$$E_{NF} = \frac{M_{MD}(DR) + B_{MD} - \Phi_f E_{C,MDMAX}}{1 - \Phi_f} \quad (13)$$

For the transverse direction modulus, eqs 9 and 12 are combined

$$E_{NF} = \frac{(1 - \Phi_f)}{\left[\left(\frac{1}{M_{TD}(DR) + B_{TD}} \right) - \left(\frac{\Phi_f}{E_{C,TD MAX}} \right) \right]} \quad (14)$$

Since all parameters other than Φ_f can be determined experimentally, eqs 13 and 14 are set equal to each other and the equation is solved using the quadratic equation for the fiber volume fraction, Φ_f , in the composite. This solution is given by eq 15.

$$\Phi_f = \left[\left(2 - \frac{M_{MD}(DR) + B_{MD}}{E_{C,TD MAX}} - \frac{E_{C,MDMAX}}{M_{TD}(DR) + B_{TD}} \right) \pm \left(\left(-2 + \frac{M_{MD}(DR) + B_{MD}}{E_{C,TD MAX}} + \frac{E_{C,MDMAX}}{M_{TD}(DR) + B_{TD}} \right)^2 - 4 \left(1 - \frac{E_{C,MDMAX}}{E_{C,TD MAX}} \right) \left(1 - \frac{M_{MD}(DR) + B_{MD}}{M_{TD}(DR) + B_{TD}} \right) \right)^{0.5} \right] \bigg/ 2 \left(1 - \frac{E_{C,MDMAX}}{E_{C,TD MAX}} \right) \quad (15)$$

The solution to eq 15 that is positive, yet less than unity should be used at draw ratios greater than the critical draw ratio, as shown in Figure 4.

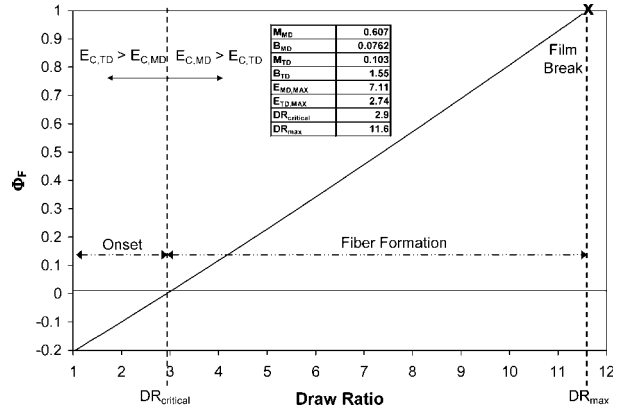


Figure 4. Plot of the model’s calculation of the volume fraction of fibers (Φ_f) of a blown high molecular weight homopolymer polyethylene film relative to draw ratio. The volume fraction of fibers was calculated from experimental data (Figs. 2 and 3). Typically, blown films are more oriented in the transverse direction, relative to the machine direction. As a result, the film has a higher transverse direction modulus. When analyzed with this model, films with this morphology have a positive volume fraction of fibers oriented in the transverse direction [Fig. 1 (a)] resulting in a negative volume fraction of fibers oriented in the machine direction (Fig. 4: for $DR < DR_{critical}$). At the critical draw ratio, which is defined as the draw ratio where the machine direction modulus is equivalent to the transverse direction modulus, the volume fraction of fibers is equal to zero, indicative of an isotropic system. Beyond this critical draw ratio, fiber formation occurs linearly with respect to draw ratio, resulting in the machine direction modulus being greater than the transverse direction modulus. Below the critical draw ratio, the transverse direction modulus is greater than the machine direction modulus, implying the absence of fibers oriented in the machine direction with reinforcing capabilities, making this model inapplicable at these conditions.

Figure 4 shows the volume fraction of fibers, relative to the draw ratio, calculated with experimental data for a blown high molecular weight homopolymer polyethylene film that has been machine direction oriented (MDO) in the solid state ($T_{orientation} < T_{melt}$). Beyond this critical draw ratio, the area of validity for this model, the volume fraction of fibers increases linearly until the volume fraction of fibers reaches unity prior to the ultimate draw ratio, at which point the film breaks.

At low draw ratios, below 3.0 for this particular film represented in Figure 4, the volume fraction of fibers calculated by this model is a small negative fraction. This is the direct result

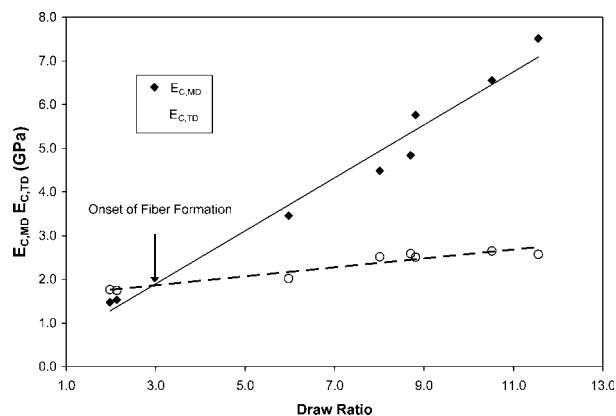


Figure 5. Plot of the experimentally measured machine direction and transverse direction moduli versus draw ratio for oriented samples of HMW-PE 1. The linear trends were generated from experimentally measured moduli values of a high molecular weight homopolymer polyethylene films that were oriented in the machine direction in the solid state. This data was used to generate the curve in Figure 4 by simultaneously solving eqs 13 and 14. Similar trends were seen with four other oriented samples of HMW-PE.²⁶

of the morphology created by the blown film process, where the transverse direction modulus ($E_{C,TD}$) is typically higher than the machine direction modulus ($E_{C,MD}$). Figure 5 is a plot of the experimentally measured $E_{C,MD}$ and $E_{C,TD}$ values with respect to draw ratio. Such a relationship between the machine and transverse direction moduli has been previously measured and reported by Ward⁴¹ and Gupta et al.⁴⁵ The linear trends also correlate well with those found in the literature.^{41,45–47}

Figure 6 shows the increase in volume fraction of fibers for five different HMW-PE films relative to the reduced draw ratio, $(DR - DR_{critical})$. Data for Figure 6 was calculated using the proposed model and experimental data,²⁶ part of which (HMW-PE 1) was presented in Figure 5 and used to generate Figure 4. The characteristics of the five different polymers used to produce the oriented films represented in Figure 6 are given below in Table 1.²⁶

Relating the Machine Direction Break Stress ($\sigma_{C,MD}^*$) and strain ($\epsilon_{C,MD}^*$) to the Volume Fraction of Fibers

The ultimate properties of the drawn sample are strongly dependent on the volume fraction of fibers created during the orientation process.

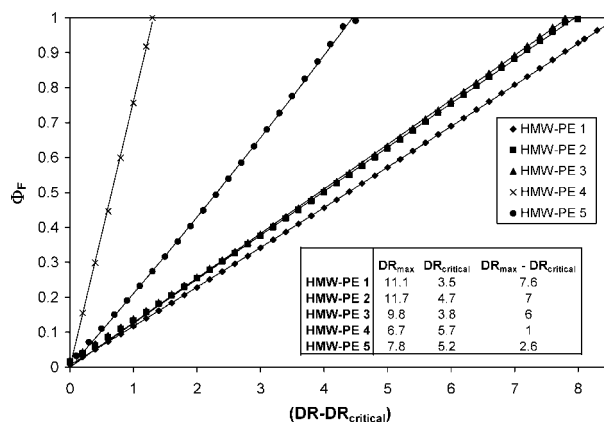


Figure 6. Plot of the volume fraction of fibers in oriented HMW-PE films relative to reduced draw ratio. The volume fraction of fibers increases from a value of zero at $(DR - DR_{critical}) = 0$ to a value of 1 prior to the film failing during the orientation process. Markers represent values calculated from simultaneously solving eqs 13 and 14 with relationships derived from experimentally measured machine and transverse direction moduli.

For example, the ultimate break strength of the oriented sample in the machine direction ($\sigma_{C,MD}^*$), which is the ultimate strength of the sample after it has been subjected to the orientation process, is linearly related to the total volume fraction of fibers.⁴⁴

$$\sigma_{C,MD}^* = \sum_{i=1}^n \sigma_i^* \Phi_i \quad (16)$$

where $\sigma_{C,MD}^*$ is the composite machine direction break stress, σ_i^* is the break stress of the i th component, and Φ_i is the volume fraction of the i th component.

On the basis of the previous fiber/nonfibrous gel discussion, for an oriented sample with a

Table 1. Characteristics of the Five Polymers Used to Produce the Oriented Films Represented in Figure 6

Film	Density (g/cm ³)	M_n	M_w
HMW-PE 1	0.959	1.29×10^4	2.07×10^5
HMW-PE 2	0.949	1.43×10^4	1.95×10^5
HMW-PE 3	0.949	1.26×10^4	2.12×10^5
HMW-PE 4	0.940	1.61×10^4	1.75×10^5
HMW-PE 5	0.938	1.83×10^4	2.09×10^5

Included are polymer density, number, and weight average molecular weights.

fixed volume fraction of fibers, eq 16 simplifies to

$$\sigma_{C,MD}^* = \Phi_F \sigma_F^* + (1 - \Phi_F) \sigma_{NF}^* \quad (17)$$

For fiber composites where the fiber component is infinitely long and perfect adhesion is assumed between the fiber and the matrix, the fiber dominates the strength of the material. The machine direction break strain is given by:⁴⁴

$$\varepsilon_{C,MD}^* = \varepsilon_F^* \quad (18)$$

where $\varepsilon_{C,MD}^*$ is the composite machine direction break strain, ε_F^* is the break strain of the fiber. When a composite behaves as an inelastic material, it will only deform to the extent that the fibrous component can elongate, as shown in eq 18. Beyond this point, the fiber breaks and the composite fails due to the significantly lower break strength of the weaker gel region.⁴⁴ In cases where the fiber is rigid and oriented in the direction of the applied stress, the elongation is minimal and approaches zero for a perfectly oriented inelastic material. At the maximum draw ratio, where $\Phi_F = 1$, the composite of this model consists of only inelastic fibrous structures perfectly oriented in the machine direction. Applying this boundary condition, eq 18 becomes

$$\varepsilon_{C,MD}^* = 0 \quad (19)$$

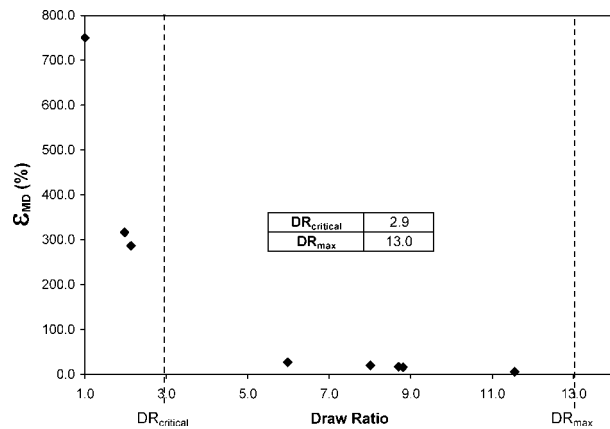


Figure 7. Plot of machine direction break strain of a blown bimodal high molecular weight high density polyethylene film versus draw ratios. At draw ratios below the critical draw ratio, the films have high machine direction break strains, indicative of its ability to plastically deform prior to failure. At draw ratios greater than the critical draw ratio, fibrillation has begun, resulting in the film behaving as a rigid, inelastic material.

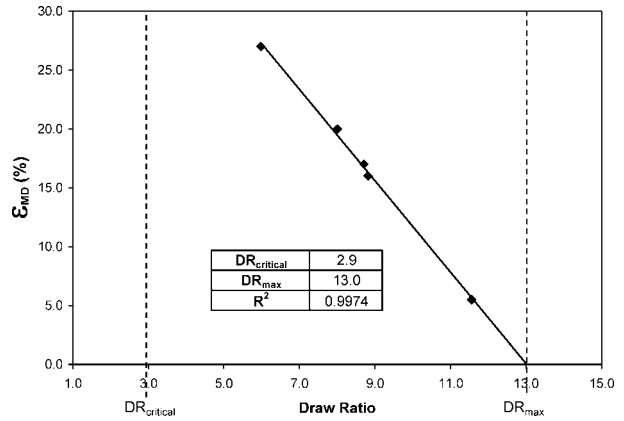


Figure 8. Plot of machine direction break strain versus draw ratio at draw ratios greater than the critical draw ratio. Between the critical and maximum draw ratio, the machine direction break strain decreases linearly with increasing draw ratio. At the maximum draw ratio, fibrillation is complete ($\Phi_F = 1$) and the film resists any plastic deformation, resulting in a machine direction break strain of zero.

At draw ratios less than the critical draw ratio, fibrous components are not present, thus they do not dominate the mechanical properties of the composite. This means the system can deform plastically and has significantly higher machine direction break strains. Beyond the critical draw ratio, the point where fibrillation begins, the fibers begin to dominate the mechanical properties of the composite, resulting in significantly lower machine direction break strains. Figure 7 is a plot of the machine direction break strains of a blown bimodal high molecular weight high density polyethylene film drawn to various draw ratios.

Experimental data shows a linearly decreasing relationship between the machine direction break strain and increasing draw ratio, as shown in Figure 8 and represented in eq 20.

$$\varepsilon_{C,MD} = M_{\varepsilon,MD}(DR) + B_{\varepsilon,MD} \quad (20)$$

PRACTICAL APPLICATION OF THE FIBER/GEL COMPOSITE TRANSITIONAL MODEL

In most commercial orientation operations, it is difficult to determine the maximum draw ratio and tensile properties of an oriented polymer film without significant experimentation. Typically, the researcher must orient the film to various draw ratios, and eventually to the point

where the film breaks. This procedure is undesirable, as it requires significant cost and time to conduct. It would be beneficial to conduct a minimum number of trials and use the mechanical data from those few samples to predict the ultimate properties of the oriented film. In addition, it would be useful to determine parameters specific to particular polymer films and orientation conditions that allows the researcher to properly select the appropriate polymer and process conditions to attain a desired set of physical properties. Such parameters include $E_{F,MD}$, E_{NF} at a specified draw ratio, DR_{max} , $DR_{critical}$, and the rate of fibrillation ($\delta\Phi_F/\delta DR$). Critical operating conditions include orientation temperature, draw ratio, and draw rate.

The first step to utilizing this model is to orient the film at two draw ratios at the same orientation conditions. These draw ratios should be high enough such that they are greater than the critical draw ratio. Tensile testing, including machine and transverse direction moduli and machine direction break stress and strain, are conducted. Next, a linear regression is used to best fit the moduli and break strain data with draw ratio. Doing so provides the parameters of eqs 11, 12, and 20 of the model. The critical draw ratio, the draw ratio where $\Phi_F = 0$, can now be calculated as the draw ratio where the linear trends for the machine and transverse direction moduli are equal. The moduli at $DR_{critical}$ is also equivalent to the modulus of the gel (E_{NF}) prior to the onset of any fibrillation, as indicated in eqs 3 and 5. One must now confirm that the two draw ratios at which the film was collected are greater than the critical draw ratio for determination of the maximum draw ratio. If they are not, samples from higher draw ratios must be obtained.

Next, a linear regression is used to fit the break strain data to draw ratio. The maximum draw ratio is now determined by extrapolating the linear relationship, as given by eq 20, to 0% break strain. Equations 11 and 12 can now be used to determine the moduli of the fibrous component in the machine and transverse direction at the maximum draw ratio. The rate of fibrillation can also be calculated, as the conditions of the critical and maximum draw ratios have now been determined.

Equation 15 can now be utilized to determine the volume fraction of fibers at a specified draw ratio, which in turn can be used to determine

the modulus of the nonfibrous gel at various draw ratios through eq 13 or 14.

Our current research is focused on understanding how polymer characteristics, such as molecular weight, molecular weight distribution, branching size and distribution, and secondary bonding (such as hydrogen bonds) effect the kinetics of fibrillation. Of specific interest are understanding inherent polymer characteristics on the critical and maximum draw ratios, the maximum moduli, rate of fibrillation, and the relationship between the moduli of the nonfibrous gel relative to draw ratio. Such information will be critical for developing polymers and films specifically for orientation processes.

FUTURE RESEARCH

In future work, the transient properties of the polymer and variations in processing conditions will be related to the properties of the structural components and incorporated into this generalized model. To do so, recent work within the literature may be utilized. The model proposed by Hong et al.^{48,49} could provide insight into the dynamics of changes in the nonfibrous gel. Additional work by Hong et al. may be useful for understanding the effects of orientation on the amorphous component, such as tie molecules, of semicrystalline polymers.⁵⁰ Techniques describe by Yamauchi⁵¹ could be incorporated to explain the thermodynamics of the fibrillation process. The methodology of Martins and Cakmak⁵² may be utilized to understand the effects of processing conditions on the fibrillation transformation process, as well as the properties of each phase. Research by Wendlandt et al.^{53,54} and Martins and Cakmak⁵⁵ may possibly be combined to understand the effects of orientation on a networked system and how that relates to the properties of the nonfibrous gel and the rate of fibrillation.

CONCLUSIONS

The transitional model presented in this article, is unique in that enhancements in the oriented sample's properties are the direct result of both the increase in the volume fraction of fibers and the change in the properties of the gel domain by transforming the less rigid components of the

non-fibrous gel into fiber-like structures at lower draw ratios. Doing so leaves stiffer components in the continuous domain and results in a gel domain with overall higher moduli at higher draw ratios. The proposed transitional model is a simple and practical way of predicting the physical properties of oriented polymer samples relative to draw ratio. By conducting a minimal amount of experimentation, detailed information about the structure and properties of an oriented film can be obtained.

The model offers a means to directly relate morphological features to the inherent properties of a polymer enabling to the development of new polymers for oriented film applications.

REFERENCES AND NOTES

- Breese, D. R.; Beaucage, G. *Curr Opin Mater Sci* 2005, 8, 439–448.
- Takayanagi, M. *Mem Fac Eng Kyushu Univ* 1963, 23, 41–96.
- Smith, J. B.; Davies, G. R.; Cappaccio, G.; Ward, I. M. *J Polym Sci Polym Phys Ed* 1975, 13, 2331–2343.
- Hosemann, R. *J Appl Phys* 1963, 34, 25–41.
- Halpin, J. C.; Kardos, J. L. *J Appl Phys* 1972, 45, 2235–2241.
- Ashton, J. E.; Halpin, J. C.; Petit, P. H. *Primer on Composite Materials Analysis*; Technomic: Stamford, Connecticut, 1969; pp 77–85.
- Gibson, A. G.; Davies, G. R.; Ward, I. M. *Polymer* 1978, 19, 683–693.
- Barham, P. J.; Arridge, R. G. C. *J Polym Sci Polym Phys Ed* 1977, 15, 1177–1188.
- Peterlin, A. *Adv Chem Ser* 1975, 142, 1–13.
- Peterlin, A. *J Mater Sci* 1971, 6, 490–508.
- Peterlin, A. *J Macromol Sci Polym Phys Ed* 1975, 11, 57–87.
- Weeks, N. E.; Porter, R. S. *J Polym Sci Polym Phys Ed* 1974, 12, 635–643.
- Cox, H. L. *Br J Appl Phys* 1952, 3, 72–79.
- Peacock, A. J. *Handbook of Polyethylene Structures, Properties, and Applications*; Marcel Dekker, Inc.: New York, 2000; Chapter 8, pp 432.
- Fischer, E. W.; Goddar, H.; Schmidt, G. F. *J Polym Sci Part A-2: Polym Phys* 1969, 7, 37–45.
- Araimo, L.; DeCandia, F.; Vittoria, V.; Peterlin, A. *J Polym Sci Polym Phys Ed* 1978, 16, 2087–2103.
- Tanigami, T.; Cho, M. H.; Kyu, T. *Eur Polym J* 1995, 7, 671–676.
- Russo, R.; Vittoria V. *J Appl Polym Sci* 1996, 60, 955–961.
- Matsuo, M. In *Oriented Polymer Materials*; Fakirov, S., Ed.; Wiley: New York, 1998; Chapter 10, pp 302–330.
- Krisyuk, B. E.; Popov, A. A.; Zaikov, G. E.; de Candia, F.; Vittoria, V.; Russo, R. *Colloid Polym Sci* 1987, 265, 220–225.
- Samuels, R. *J Polym Sci Part A: Gen Pap* 1965, 3, 1741–1763.
- Kaito, A.; Nakayama, K.; Kanetsuna, H. *Polym J* 1982, 14, 757–766.
- Kaito, A.; Nakayama, K.; Kanetsuan, H. *J Appl Polym Sci* 1985, 30, 1241–1255.
- Zubov, Y. A.; Chvalun, S. N.; Selikhova, V. I.; Konstantinopolskaya, M. B.; Bakev, N. *Polym Eng Sci Mid-September* 1992, 32, 1316–1324.
- Matsuo, M.; Ooki, J.; Harashina, Y.; Ogita, T.; St. John Manley, R. *Macromolecules* 1995, 28, 4951–4960.
- Breese, D. R.; Beaucage, G. *J Polym Sci*, Unpublished work.
- Bassett, D. C.; Carder, D. R. *Philos Mag* 1973, 28, 535–545.
- Schellenberg, J. *Adv Polym Technol* 1997, 16, 135–145.
- Peacock, A. J. *Handbook of Polyethylene Structures, Properties, and Applications*; Marcel Dekker, Inc.: New York, 2000, Chapter 5, pp 133.
- Keller, A.; Machin, M. J. *J Macromol Sci B (Physics)* 1967, 1, 41–91.
- Zhang, X. M.; Elkoun, S.; Aji, A.; Huneault, M. A. *Polymer* 2004, 45, 217–229.
- Van Der Heijden, P.; Bouzenad, F.; Diat, O. *J Polym Sci Part B: Polym Phys* 2004, 42, 2857–2870.
- Brady, J. M.; Thomas, E. L. *J Mater Sci* 1989, 24, 3311–3318.
- Bowden, P. B.; Young, R. J. *J Mater Sci* 1974, 9, 2034–2051.
- Tagawa, T. *J Polym Sci* 1980, 18, 971–979.
- Matsumoto, T.; Kawai, T.; Maeda, H. *Die Makromolekulare Chemie* 1967, 107, 250–252.
- Peacock, A. J. *Handbook of Polyethylene Structures, Properties, and Applications*; Marcel Dekker, Inc.: New York, 2000; Chapter 8, pp 415–458.
- Christ, B.; Mirabella, F. M. *J Polym Sci Part B: Polym Phys* 1999, 37, 3131–3140.
- Koenig, J. L.; Cornell, S. W.; Witenhafer, D. E. *J Polym Sci Part A-2: Polym Phys* 1967, 5, 301–313.
- Zhou, H.; Wilkes, G. L. *J Mater Sci* 1998, 33, 287–303.
- Ward, I. M. *Plastics Rubber Process Appl* 1984, 4, 77–83.
- Karasawa, N.; Dasgupta, S.; Goddard, W. A. *J Phys Chem* 1991, 95, 2260–2272.
- Buckley, C. *Ann Rev Mater Sci* 1995, 25, 295–323.
- Agarwal, B. D.; Broutman, L. J. *Analysis and Performance of Fiber Composites*; Wiley: New York, 1990; Chapter 3, pp 54–120.
- Gupta, V. B.; Keller, A.; Ward, I. M. *J Macromol Sci Phys* 1968, 1, 139–146.

46. Capaccio, G.; Crompton, T. A.; Ward, I. M. *J Polym Sci Polym Phys Ed* 1980, 18, 301–309.
47. Capaccio, G.; Ward, I. M. *Polymer* 1974, 15, 233–238.
48. Hong, K.; Rastogi, A.; Strobl, G. *Macromolecules* 2004, 37, 10174–10179.
49. Hong, K.; Rastogi, A.; Strobl, G. *Macromolecules* 2004, 37, 10165–10173.
50. Hong, K.; Strobl, G. *Macromolecules* 2006, 39, 268–273.
51. Yamauchi, T. *J Appl Polym Sci* 2006, 100, 2895–2900.
52. Martins, C. I.; Cakmak, M. *Polymer* 2007, 48, 2109–2123.
53. Wendlandt, M.; Tervoort, T. A.; Suter, U. W. *Polymer* 2005, 46, 11786–11797.
54. Wendlandt, M.; Tervoort, J. D.; van Beek, T. A.; Suter, U. W. *J Mech Phys Solids* 2006, 54, 589–610.
55. Martins, C.; Cakmak, M. *Macromolecules* 2006, 39, 4824–4833.